The expansion of tree plantations across tropical biomes

Matthew Fagan (mfagan@umbc.edu)
Department of Geography and Environmental Systems, University of Maryland, Baltimore County
https://orcid.org/0000-0002-8023-9251

Do-Hyung Kim
United Nations Children's Fund

Wesley Settle
Department of Geography and Environmental Systems, University of Maryland, Baltimore County

Lexie Ferry
Department of Geography and Environmental Systems, University of Maryland, Baltimore County

Justin Drew
Department of Geography and Environmental Systems, University of Maryland, Baltimore County

Haven Carlson
Department of Geography and Environmental Systems, University of Maryland, Baltimore County

Joshua Slaughter
Department of Geography and Environmental Systems, University of Maryland, Baltimore County

Joshua Schaferbien
Department of Geography and Environmental Systems, University of Maryland, Baltimore County

Alexandra Tyukavina
University of Maryland

Nancy Harris
World Resources Institute

Elizabeth Goldman
World Resources Institute

Elsa Ordway
Harvard University

Article

Keywords:

Posted Date: June 22nd, 2021

DOI: https://doi.org/10.21203/rs.3.rs-604751/v1

Abstract

Across the tropics, recent agricultural shifts have led to a rapid expansion of tree plantations, often into intact forest and grassland habitats. However, this expansion is poorly characterized. Here we report tropical tree plantation expansion between 2000 and 2012, based on classifying nearly 7 million unique patches of observed tree cover gain using optical and radar satellite imagery. Most observed gain patches (69.2%) consisted of small patches of natural regrowth (5.9 ± 0.2 Mha). However, expansion of tree plantations dominated observed increases in tree cover across the tropics (11.8 ± 0.2 Mha) with 92% of plantation expansion occurring in biodiversity hotspots and 14% in arid biomes. We estimate that tree plantations expanded into 9.2% of accessible protected areas across the humid tropics, most frequently in southeast Asia, west Africa, and Brazil. Given international tree planting commitments, it is critical to understand how future tree plantation expansion will affect remaining natural ecosystems.

One Sentence Summary: Tree plantations dominated recent expansions of tropical tree cover, including into 9% of accessible parks in the humid tropics.

Main Text

Over the last several decades, the expansion of commercial agriculture has become one of the key drivers of rainforest loss (*1*, *2*). Concurrently, agricultural production in tropical biomes has undergone a dramatic shift that has led to increases in the production of crops and wood products from tree plantations (*3*, *4*), defined here as productive monocultures composed of erect trees. Numerous studies have reported regional expansions in agricultural tree crops (e.g., banana, oil palm, rubber; (*5*, *6*) and in timber and pulp plantations (e.g., pine, eucalyptus; (*7*, *8*)). This expansion of tree plantation area has frequently come at the expense of intact forest and grassland habitat (*5*– *7*, *9*). Despite this risk, many countries have prioritized expanding tree plantations as part of their international commitments to restore degraded tropical habitats (*10*, *11*). For example, 45% of national commitments to the Bonn Challenge, an international goal to restore 350 million hectares of land by 2030, consist of expanding tree plantations (*12*).

Despite the availability of national statistics to document these trends, consistent, spatially-explicit estimates of global increases in tree plantation area are lacking (*13*– *15*). Many efforts to map tree plantations rely on manual delineation of tree plantation boundaries from high-resolution satellite imagery and/or field-collected data (*1*, *14*, *16*– *18*). These expert delineations cannot consistently detect changes in tree plantation area across regions because they focus on areas of intensive production and on a single time period. For example, although a recent study of tropical humid forest change ostensibly tracked plantation expansion over time, its delineation of tree plantations largely relied on single-date expert interpretation and the plantation map accuracy was not reported (*18*).

The absence of systematic monitoring of plantation expansion complicates assessments of both forest restoration efforts and the impacts of tree plantations on conservation. Confusion between natural

forests and tree plantations in forest change maps leads to “cryptic forest loss” (*19*) and/or overestimates of natural forest loss and recovery (*20*, *21*). This is especially true in the tropics, with its rapid tree growth and expansion of tree plantations. National reporting indicates net increases in tree plantation cover of 1-2% a year (*22*), but tracking net changes in the area of frequently disturbed land covers like tree plantations and natural forest regrowth can underestimate the occurrence of expansion in new areas as existing areas are harvested. According to the FAO, the area of planted forests (239 million ha) and permanent (i.e., perennial) crops (169 million ha) in 2020 was much smaller than that of natural forest cover regenerating from disturbances (3.75 billion ha) (*22*, *23*). However, given that the FAO definition of naturally regenerating forest includes existing, selectively logged forests, it remains unclear whether natural forest recovery or tree plantations are driving expansions in global tree cover.

To address these uncertainties, we undertook a pantropical assessment of increases in tree plantation area, with tree plantations defined here as monocultures of agricultural or industrial tree species established and managed by humans for fruit, wood, fiber, and other products. We focused on the tropics (25° N to 25° S) due to the prevalence of natural forest conversion to commodity tree crops across tropical latitudes (*1*) and high rates of potential carbon sequestration from tropical tree regrowth (*24*). Our aim was to use remote sensing data to accurately distinguish plantation expansion from natural forest regrowth, and assess recent expansion across tropical biomes, biodiversity hotpots, and protected areas.

Monitoring plantation expansion

Mapping tree plantations consistently using satellite data is challenging, especially using the moderate spatial resolution imagery (10 to 100 m) needed for comprehensive regional coverage. This challenge arises in part from spectral and structural similarities between regrowing natural forest and plantations of trees (*25*–*27*). Tree plantations are spectrally diverse, with substantial variation in spectral signatures across species, age classes, planting pattern and density, nutrition and disease status, soil types, understory cover, and disturbance intensities (*25*, *28*, *29*). Regrowing forests are also spectrally and structurally diverse, for similar reasons, especially across distinct forest types (*30*, *31*). These similarities, coupled with geographic variation in spectral reflectance and phenology, and persistent tropical cloudiness, make it difficult to consistently distinguish tree plantations from natural forest using satellite imagery (*5*).

Although intra- and inter-regional plantation variability has limited accuracy at larger scales, maps based on automated classification of remotely sensed imagery have successfully monitored plantation expansion at regional scales (e.g., (*5*)). However the accuracy of regional tree plantation maps differs widely across different geographies and plantation species (*5*, *14*). In general, extensive monocultures of non-native plantation species have been more readily distinguished, especially if they possess distinct spacing or phenology. For example, rubber and oil palm have been mapped with intermediate to high accuracy (80-90+%) at local to near-global scales (*5*, *32*–*35*). However, other tree crop and timber species often are mapped with lower accuracy: in Brazil and Chile, country-level mapping of non-native eucalyptus and pine plantations has had intermediate levels of accuracy (70-89%) (*16*, *36*).

Research Design

In this study, we integrated two different types of satellite imagery, optical and microwave, to better characterize the spectral (optical) and structural (microwave) properties of regrowing tree plantations and natural forests. To estimate recent increases in plantation area and in natural forest regrowth, we reclassified a widely used map of gains in tree cover between 2000 and 2012 (*37*), the Global Forest Change (GFC) product. From this dataset, we selected mapped gain patches ≥0.45 ha in size that persisted for three full years after 2012, through the end of 2015 (n=6,901,681). Over each resulting patch of gain pixels, we extracted spectral and microwave satellite imagery data (Landat, ALOS PALSAR-2, and Sentinel-1) and other ancillary data (e.g., GFC tree cover, patch size and shape; table S1) for a total of 32 metrics per patch (table S1).

We then used machine learning to predict patch-level land use in 2015. The output was a classification of gain patches as either “tree plantation”, “natural regrowth”, or “open” (<10% tree cover); these classes characterize increases in tree cover between 2000 and 2012 that persisted through 2015. Then, to assess the extent of plantation expansion across the tropics, classified gain footprints were intersected with available spatial data on biomes, biodiversity hotspots, national borders, and protected areas.

Product Accuracy

We assessed the classification accuracy of the resulting map of plantation expansion. Model accuracy was independently evaluated by random sampling of 2000 gain patches across the tropics. For each reference patch, high-resolution imagery was used to determine a patch land-use class; reference patches with mixed land-uses were assigned to a class using percent cover rules (e.g., majority percent cover; table S5). Overall map accuracy (OA) was 90.6% (±0.1; table S6), with the largest error in the open class, and high mean class accuracies for plantation (93.1%) and natural regrowth (87.0%). This far exceeds the accuracy of a recent tropical moist forest product (*18*), which we estimate mapped just 60.2% of our reference plantation patches correctly (table s9). Latin America and Africa had the highest classification accuracies (table S6), with somewhat lower overall accuracy in Asia (89.7% OA) where misclassification of natural regrowth as plantation was highest.

Global expansion patterns

Between 2000 and 2012, persistent gain in tree cover associated with tree plantations was nearly double the persistent gain in tree cover associated with natural forest regrowth. Pantropically, there were at least 11.8 (±0.2) Mha of additional tree plantations and 5.9 (±0.2) Mha of additional natural regrowth (Table 1, Figures 1, s4-s9). Although patches of natural regrowth far outnumbered plantation patches, individual plantation patches were ~4.8x larger than areas of forest regrowth (Table 1). Across continental regions, tree plantations increased across the most area in Asia, followed by Latin America (Table 1). Africa had the smallest plantation expansion and the greatest increase in natural regrowth, but plantations still made up a quarter of observed increases in tree cover there.

	Est. gain area (Mha)	Area CI (Mha)	% of region gain area	Est. patch number	Mean patch size (ha)
Region					
Africa					
Tree plantations	0.4	0.06	25.0	77,046	5.3
Natural regrowth	1.2	0.06	73.5	1,296,932	0.9
Open	0.02	0.02	1.5	23,456	1.1
Latin America					
Tree plantations	3.3	0.12	58.6	499,042	6.6
Natural regrowth	2.1	0.12	37.7	1,549,391	1.4
Open	0.2	0.05	3.7	88,832	2.3
Australasia					
Tree plantations	8.1	0.13	75.6	1,415,054	5.7
Natural regrowth	2.6	0.12	24.1	1,928,709	1.3
Open	0.03	0.02	0.3	23,219	1.4
Tropics					
Tree plantations	11.8	0.19	65.7	1,991,142	5.9
Natural regrowth	5.9	0.18	32.8	4,775,032	1.2
Open	0.3	0.05	1.5	135,507	1.9

Table 1. Estimated expansion area of tree plantations and natural regrowth, 2000-2012, including the area of mapped tree cover gain estimated to be not forested ("Open").

Our findings show that expansion of tropical tree plantations primarily occurred in the humid tropical biome (Figure 2). However, new plantations were a common (14% of total global plantation area) and dominant form of increasing tree cover (73% of observed regrowth) in arid tropical biomes in eastern Africa and southeast Latin America, matching concerns about recent afforestation in arid regions (*38*, *39*). Furthermore, plantation expansion was concentrated in designated biodiversity hotspots, and particularly the Sundaland (southeast Asia), Cerrado (southern Brazil), and Atlantic Forest (southeast Brazil) hotspots (collectively 92.8% of total plantation area; fig. S10). By contrast, natural regrowth was relatively evenly distributed among biomes and hotspots, although natural regrowth was slightly more abundant, and plantations less abundant, in ecoregions with high remnant natural forest cover (Table S10, $p<0.0001$)

We show that plantation expansion was concentrated (82.8%) in four large countries (Indonesia, Brazil, Malaysia, and China), but tree plantations were widespread, occurring in 78 of 112 tropical countries with detected increases in tree cover (table S11). Relative to natural regrowth, tree plantation patches were distributed in a distinct geographic manner. Tree plantation expansion was more likely than natural

regrowth to be found near navigable waterways ($p<0.0001$, fig. s11a), likely reflecting the role of global trade in influencing the expansion of plantations. Similarly, tree plantations were more likely to be found in highly human-dominated landscapes than natural regrowth ($p<0.0001$, fig. s11b).

Expansion in protected areas

Tree plantation expansion into protected areas was relatively uncommon across the tropics, affecting 4.2 percent of protected areas (PAs) (PAs with ≥5 ha of expansion) (table S12). However, expansion was more common in PAs located in the humid tropical biome (5.5% of PAs) especially in PAs there with above-average accessibility and human influence (9.2% of affected PAs). Furthermore, plantation expansion often occurred in close proximity to tropical protected areas (<1 km outside), affecting 7.8% of all PAs, 11.4% of humid tropical biome PAs, and 16.2% of humid PAs with high human influence (tables S12, S13). Notable concentrations of plantation expansion into protected areas include southeast Asia, southeast Brazil, and western and eastern Africa (Figure 2). Plantation expansion was rarely widespread within protected areas, with only 2.1% of PAs experiencing ≥50 ha of tree planation expansion. But where it occurred inside protected areas, plantation expansion was a dominant mode of increasing tree cover, making up 49.5% (± 38.5%, s.d.) of observed gains in cover within affected protected areas. In Africa, parks with stricter protected status (IUCN category) were less likely to experience plantation expansion ($p<0.0001$; table S14). However in Latin America and Asia, protected status was unrelated to the presence of plantations within parks ($p>0.05$), potentially reflecting greater encroachment pressure in these regions.

Product limitations

There are several known limitations of this product. First, its accuracy in characterizing increases in tree cover depends on the accuracy of the original GFC product (*37*). The original product contained relatively high errors of omission in predicting tropical tree cover gain (capturing ~50% of observed gain). Because of potential differences in detectability, it is possible that either tree plantations or natural regrowth are relatively more abundant in the omitted tree cover gain. To test this hypothesis, we conducted an independent random assessment of changes in humid tropical tree cover (n=3000) and found that plantations made up at least 45.5% of tree cover increases, with no observed bias in GFC detection of plantations (table S15). Taken together, our results clearly indicate that tree plantation expansion is widespread across all tropical regions and biomes. The observed relative dominance of plantations does not arise solely from differential persistence of detected plantations and natural regrowth over time, or from patch size thresholds, as estimated plantation expansion is at least 40.4% of the original GFC gain area (fig. s12). Furthermore, the number of natural forest regrowth patches markedly exceeds the number of plantation patches in our dataset (Table 1).

The GFC product also tends to underestimate tree cover in arid biomes (*40*). Consequently, outside the humid tropical biome our product may misestimate both total tree cover gain area and the relative importance of plantations. Further, because our product was derived from both optical and microwave data, local variation in topography and forest structure affected classification accuracy. Our product

tended to have lower accuracy in mountainous areas (where microwave returns vary) and in natural regrowth patches where structure or color resembled row-planted monocultures. For example, visual inspection showed more frequent errors in open natural regrowth affected by fire or selective logging, and in single-species dominated natural regrowth patches with a smooth canopy (for example, riparian regrowth in the western Amazon). In certain cases, natural regrowth within plantations was underestimated: when mixed gain patches occurred (containing both tree plantations and natural regrowth), whole gain patches were labeled according to their majority land-use class.

When we compared our estimates of increases in plantation cover to those reported by countries to the UN Food and Agriculture Organization (FAO) between 2000 and 2010, we found that our results were lower than the FAO-reported area of timber and agricultural plantations for most countries, most notably in India and west Africa (fig. S12). However, only a fraction of FAO-reported plantation expansion was captured by the original GFC gain dataset ((*37*), fig. S12). This is likely due to both definitional differences (e.g., tea plantations in India are <5 m in height and do not meet the GFC tree cover definition) and errors of omission (table s15). Thus, our model estimates of the total area of plantation expansion are likely to be conservative.

Conclusions

Tree plantations are a key element of ambitious policy proposals to restore ecosystem services and address climate change, including the Bonn Challenge, the Trillion Tree initiatives, and the UN Decade on Ecosystem Restoration (*12*, *41*). Given their potential impacts on biodiversity, fire risk, and human well-being, tree plantations are controversial (*12*, *38*, *42*). This controversy has largely proceeded in the absence of global data on plantation expansion, and the net impact of plantation expansion has thus been difficult to assess, especially in understudied regions like Africa. In this context, our findings provide a few useful insights for future policy and research.

First, tree plantations make up a large proportion of recent increases in tropical tree cover. This indicates that many global- and country-level estimates of tropical forest loss and gain are potentially biased by the presence of tree plantations, which have disturbance rates distinct from those of natural forests. Distinguishing tree plantations from natural regrowth enables assessments of their relative persistence over time (*43*), the spatiotemporal clustering of expansion and replanting (*13*), and the displacement of previous land uses by plantation expansion (*44*).

Second, the abundance of natural forest regeneration relative to plantations was much lower than predicted by nationally reported statistics, suggesting that they do not accurately track forest expansion through natural regrowth. This is most likely because the area of selectively logged tropical forest far exceeds that of natural regrowth (*45*), but may also result in part from rapid re-clearing of natural regrowth (*43*). Understanding the fate of the large number of natural regrowth patches identified here is critical to determining the long-term climate mitigation potential of tropical forests (*46*). Using data on

tree height (*47*) and carbon uptake (*24*, *48*), future research could estimate annual carbon sequestration rates for tree plantations and natural regeneration during this period.

Third, the widespread expansion of plantations into arid biomes and tropical protected areas indicate that economic considerations frequently took precedence over conservation policies and interests during this time period. The net benefits of planting trees—for carbon, biodiversity, and food security—entirely depend on the types of ecosystem they replace (*49*). Thus, tracking plantation expansion is essential to improve estimates of net global carbon sequestration and available agricultural area, and to assess the net impacts of progress towards restoration commitments. Using new data on tropical forest loss and regrowth (*18*), products like this one could be annually updated. Given current widespread international interest in tree planting, it is critical to monitor going forward how proposed expansions in plantation cover will affect remaining natural ecosystems.

Materials And Methods:

Study region and patches: We focus on recent areas of increase in tree cover, or "gain", between the years 2000 and 2012, delineated in a previous study of global forest change ((*37*); Global Forest Change (GFC) data version 1.5). We examined all mapped patches of contiguous gain pixels (30 m resolution) between 25 degrees North and South that met our minimum patch size criteria (≥ 0.45 ha). Then, because our preliminary analysis indicated that false-positive identification of tree cover gain was more common in small patches and in patches that showed ephemeral vegetative gain (gains followed by losses), we set criteria for minimum forest persistence. We selected only gain patches >0.45 ha in size that persisted at least four years after 2012. These minimum patch size and persistence criteria acted as a conservative forest filter, eliminating non-forest error patches, and their derivation is described in more detail in the Supplementary Materials. Contiguous gain patches were generated, updated by removing forest loss, and converted to polygons in Google Earth Engine (GEE), with a unique ID number assigned.

Patch-level data: For each resulting gain patch (n= 6,904,335), several characteristics were calculated, including patch area, patch perimeter length, the patch perimeter: area (P:A) ratio, and a patch compactness index based on area and perimeter (*50*). In addition, two additional patch metrics were derived: the distance to the nearest patch with a high P:A ratio (i.e., in the top 1% of patches), and the distance to the nearest patch with a high compactness index (i.e., in the top 1% of patches). Patch characteristics were calculated in the native projection of the original raster dataset (WGS-84) using the sf and geosphere packages in R version 3.5.1.

To distinguish natural regrowth and tree plantations, we used two different types of coincident satellite remote sensing data: optical and radar data. Moderate-resolution Landsat optical imagery have been used for many studies of forest and land cover due to the availability of free, consistent observations over several decades (*14*, *37*). However, as an optical sensor, Landsat data are severely influenced by the presence of clouds, particularly in the tropics (*51*, *52*). Furthermore, the spectral resolution of single-date Landsat data has often not been sufficient by itself to separate forest and tree plantations (*14*, *53*).

Radar data, in contrast, are less sensitive to cloud cover and potentially more sensitive to differences in structure between natural and anthropogenic tree cover (*54*, *55*). Although until recently radar data had relatively limited availability compared to Landsat (*54*), global mosaics of PALSAR-1 (2007-2010), PALSAR-2 (2015+), and Sentinel-1 (2014+) data are now freely available.

In this analysis, we used the global Landsat spectral mosaics available from the GLAD lab (version 1.3) (*37*), covering the entire globe for the nominal year of 2015. For coincident radar data that was as close as possible to the 2012 end date for gain patches, we used the 2015 global mosaic of L-band PALSAR-2 data available from JAXA (*56*), and a 2015 global mosaic of C-band Sentinel-1 data from the ESA (*57*). Details on optical and radar data band selection and processing are available in the Supplementary Materials.

In addition to spectral, radar, and patch-characteristic data, we included several satellite-derived land cover datasets as input data in this analysis. These data consisted of GFC tree cover in the year 2000, GFC loss year, and a 1 km dataset on crop extent (https://developers.google.com/earth-engine/datasets/catalog/USGS_GFSAD1000_V1). For each patch, we calculated the patch-level mean and standard deviation of all pixels that intersected with the patch boundary. The patch-level mean and standard deviation calculations for each band included pixels that overlapped with individual patch boundaries, but all calculations weighted individual pixels according to their area, following a standard Google Earth Engine algorithm.

The resulting dataset included 35 different variables for each individual patch (Table S1); all variables were used in further analyses. Missing Sentinel-1 or ALOS Palsar data values were detected in 0.038% of patches, mainly due to lack of data coverage over small, remote islands. These patches were omitted from further analysis and are mapped as no-data in the final dataset (final patch n= 6,901,681).

Reference data labeling: Tree plantation reference data came from two main sources: the World Resource Institute (WRI), and manual delineation of plantations. We used the WRI tree plantation polygons to select all Hansen gain polygons that intersected their boundaries, with post-intersection filtering described in the Supplementary Materials. Due to the lack of quality plantation training data in Africa, Australia, and mainland southeast Asia, we also manually delineated a variety of plantation species across these regions using freely available time series of high-resolution imagery (Google Earth, Bing, ArcGIS basemap). Gain patches were selected in this process by intersection with manually-created polygons, including only patches dominated by obvious plantation species.

Criteria for distinguishing plantation species included 1) domination by a single commercial tree species (consistent color and uniform canopy shapes) and 2) the clear presence of rows of trees at some point in the imagery time series (pattern). Clear evidence of human disturbance over time, extractive infrastructure, and regular patch edges often facilitated identification of potential plantation patches, but by itself was not diagnostic of plantations due to farm and plantation abandonment. Common commercial plantation species (oil palm, rubber, eucalyptus, pine) were recognizable and distinct in high-resolution imagery, as were many unknown plantation species in Africa and Australia. Diverse

polyspecies plantations and agroforestry stands were omitted by this methodology. We did not manually delineate plantation systems with a mixed set of species or that lacked a row structure (e.g., some agroforestry). In addition, globally rare plantation types with distinct species, cultivars, and/or conditions (e.g., insect infestation) are likely to have been omitted.

Natural forest regrowth reference data was derived from three main sources: the Intact Forest Landscapes dataset (IFL; (*58*), the World Database on Protected Areas (WDPA v1.4; (*59*)), and manual delineation of natural regrowth. The WDPA polygons were edited to include only patches clearly dominated by natural regrowth, as is described in more detail in the Supplementary Materials. Gain patches were then selected and labeled in this process by intersection with IFL, WDPA, and manually-created polygons. Our initial reference data sample, based on intact forest landscapes and protected areas, had gaps in spatial coverage of secondary forests in in southeastern Amazonia, southern Mexico, Africa, and southeast Asia. To address these gaps, we manually delineated natural regrowth patches across these regions using freely available time series of high-resolution imagery (Google Earth, Bing, ArcGIS basemap). Natural regrowth was distinguished by several criteria, including a diversity of tree crown shapes, colors, and/or sizes, irregular patch edges, the absence of human infrastructure, and/or no evidence of tree planting or rows in the imagery time series (fig. S1). Some natural stands did not meet several of these criteria, but could be distinguished from plantations by one or more attribute.

Training data processing: The resulting training data included 729,092 gain patches, consisting of natural regrowth, 15 different known plantation species, and several unknown plantation species (Table S2). Oil palm and eucalyptus dominated the initial training sample, making up 82% of all plantation training data. Plantation training data was unevenly distributed across continents, with Africa having the smallest number of samples (Table S2). By contrast, the training data for natural regrowth was more evenly distributed across continents (Table S2). With no a priori information on the relative abundance of different plantation species and natural regrowth across the globe, the initial training dataset was an unbalanced mixture of different plantation species and natural regrowth patches. To balance the training the plantation training data, we first resampling the existing data, which is described in more detail in the Supplementary Materials. We then randomly withheld 10% of the processed training data as internal validation data (n=72,908).

Second, given that the relative global proportion of plantation and regrowth was unknown, we created eleven different final training datasets through subsampling (and where necessary to increase sample size of a particular class, sampling with replacement). Each training sample was created with different proportions (balancing) of plantations and regrowth (total sample n= 559,580 – 839,370), covering a range of proportions that preliminary analysis indicated changed the predicted outcomes of classification models (Table S3; Supplementary Materials).

Machine learning classification models: For each of the 11 different balancings of the training data, we fit five types of binary classification models, totaling 55 classification models. The binary classes predicted were natural regrowth, and tree plantation, and the independent predictors are summarized in Table S1.

All classification models were implemented in the R interface to the H2O machine learning environment (https://www.h2o.ai, version 3.26.0.5), with default model parameter and grid search settings. The five types of classification models were: 1) gradient boosting machines (GBM), 2) logistic general linear models (GLM), 3) Distributed Random Forest (DRF), 4) Extremely Randomized Trees (XRT), and 5) feed-forward deep-learning neural networks (DL). To facilitate grid searches for parameter values and conduct direct model inter-comparison, we used the H2O automated machine learning (h2o.autoML) algorithm with default values (*60*). At the end of each autoML run, the most accurate model (highest AUC) for each model type was saved (see Supplementary Materials for details).

The resulting best models in terms of AUC in each of the five model families, for each of the 11 training datasets (55 models in total), were each used to predict the binary class of the internal validation data (n=72,908). The resulting predictions included the binary class prediction and the likelihood of that predicted class, which ranged from 0 to 1. The likelihood of the plantation class was selected as a variable for further analysis, with 55 total classification model predictions. All of these 55 classification model predictions, along with the internal test class labels, were used as input data to a stacked ensemble machine learning model.

Stacked ensemble classification: Stacked ensemble machine learning models (*61*) were used to predict the binary land use class (natural regrowth or tree plantation) of each patch, using all of the individual classification model predictions as input data. Stacked ensemble predictions used the Random Forest algorithm as a final classifier, with model parameters set to the H2O modeling environment defaults (ntrees=50, mtries= 7 (i.e., the square root of the number of predictor variables)). The internal validation data were used as the input labeled training data. A separate stacked ensemble model was developed for three main tropical regions: Latin America, Africa, and Australasia (Asia, Australia, and Oceania), leading to different input training data proportions for each region (Table S4). The resulting stacked ensemble models, one for each tropical region, were used to predict the binary land use class of all patches within their region.

Masking and post-processing: Post-classification analysis of the predicted product indicated two main quality issues. First, because GFC gain patches in mangrove patches were quite rare globally (*62*) and thus rare in the training data, misclassification of low-diversity mangrove gain patches as tree plantations was common in southeast Asia. To address this issue, a high-quality global mangrove extent map ((*63*); 90% overall accuracy) was used to correct our product. All gain patches that intersected with the 2015 mangrove extent were reclassified as the natural regrowth class, unless they exceeded 20 hectares in size and had less than 5% of their area overlapping the mangrove map. This low percent area threshold excluded the majority of tree plantation patches that bordered mangroves.

Second, visual inspection of the final product indicated that a small proportion of gain patches (1.3% of the independent testing data) were non-forest by 2015, with low levels of tree cover (<10% cover). Patches with low tree cover in 2015 were generally typified by low levels of greenness (patch level mean NDVI <0.48) and low biomass (patch level mean PALSAR HV decibel return <1800). Thus, these two manually-

determined thresholds were used jointly to classify gain patches with very low tree cover as a separate third land use class, Open. These thresholds readily captured bare ground and open water, but sometimes included short plantations and secondary forests in arid regions with seasonal deciduousness.

Accuracy Assessment: To permit assessment of how accurately patches of tree plantations and natural regrowth were distinguished across the tropics, we generated labeled testing data. We assessed map accuracy using randomly selected reference polygons (n=2000; Figure S2) sampled with respect to stratum weight (patch area), with replacement. Reference polygons (which consisted of whole gain polygons) were categorized into one of three broad land-use categories (natural regrowth, tree plantations, and open) for accuracy assessment, based on a set of rules evaluating percent tree cover, land use, and land cover (Table S5) for the year 2015. For the purposes of accuracy assessment, open polygons had <10% tree cover (FAO forest definition (*22*)), and reference polygons dominated by mixes of both natural regrowth and plantation land-uses were labeled as the land-use with greater cover (Table S5). This categorization scheme summarized a diversity of observed land uses, including natural regrowth, plantation, water, open agricultural land, low-density open land, partially-cleared plantations or regrowth, and mixes of patches of regrowth and plantation within a polygon. In each polygon, land use for the year 2015 was identified by two trained analysts using freely available high-resolution imagery (Google Earth, Bing, and ArcGIS Basemap).

We calculated the map area-weighted accuracy of our final predicted map for the global study area, and for each of the three study regions (Table S6) (*64*). Derived confusion matrices show the count of reference data in a particular class (Table S6), but the associated percent accuracy statistics are polygon area-corrected estimates, following Pickens et al. (*64*). Area-corrected accuracy estimates and confidence intervals were derived for the three land-uses classes, and overall accuracy. Corrected map area estimates for each land-use class were then calculated at the global and regional scales, along with area confidence intervals. For each of these combinations of region and map type, we report overall map accuracy both including and excluding very large polygons (tables S6, S7, S8).

In a separate analysis, we assessed land-use at random points (n=3000) across the humid tropical biome for the period 2000-2012. See the Supplemental Materials for details.

Patch-level analysis: Using the centroid of each patch of tree cover gain to locate patches in space, we examined the distribution of tree plantation and natural regrowth patches (figs. S4-s9) with respect to A) navigable bodies of water and B) a metric of human influence (the human impact index (HII) (*65*)). Both the 2009 HII and water map rasters were created by Venter et al. (*65*) and had a spatial resolution of 1 km^2; the water data included navigable rivers, lakes, and the ocean. A raster of Euclidian distance to the nearest navigable water was calculated using Guidos Toolbox. For each patch, we extracted A) distance to water and B) HII for the centroid point as response variables. We then tested for significant differences in the distribution of the two focal land-use classes (tree plantations and natural regrowth) using a separate Kruskal-Wallis rank sum test for each response variable.

Country-level analysis: We summarized the estimated plantation and regrowth area in each tropical country by intersecting the centroids of predicted land-use polygons with a national border database (*66*). Both polygon area and country area between 25° N to 25° S were calculated using the WGS-84 projection in the geosphere R package (*67*). We compared our estimated plantation expansion (plantation gain patches between 2000 and 2012, surviving to 2015) in each country with the area of increase in plantations and tree crops reported to the FAO for the period 2000-2010.

Biome- and hotspot-level analysis: We also summarized the estimated plantation and regrowth area in each tropical biome (*68*) and biodiversity hotspot ((*69*); version 2016.1). We intersected the centroids of predicted land-use polygons with published biome and hotspot datasets. Terrestrial hotspot areas were selected for analysis, and the biome dataset contained ecoregions as a biome subunit. Polygon area, country area, and biome area between 25° N to 25° S were calculated using the WGS-84 projection in the geosphere R package (*67*). For each biome, ecoregion, and hotspot, we calculated the total and percentage area of observed natural regrowth and tree plantation expansion. Additionally, in each ecoregion, we calculated the percent of area occupied by intact forests in 2013 ((*70*); "intact forest dominance"). To assess how well ecoregion area and intact forest dominance predicted the total area of tree plantations and natural regrowth in each ecoregion, we conducted a multiple linear regression, with all area variables log-transformed. The type of tree cover gain was a categorical predictor which interacted with ecoregional area and intact forest dominance, respectively.

Protected area analysis: Protected area data (boundary, location, and status) were derived from the 2018 World Database on Protected Areas (WDPA v1.4; (*59*)), and details on WDPA data pre-processing and analysis are available in the Supplemental Materials. To examine how tree plantation expansion and natural forest recovery affected PAs across our study region, we quantified the area of plantation and regrowth located inside PAs and outside but near PAs (≤1 km from the border). To limit the impact of misclassification error on estimates of plantation area within protected areas, only PAs containing >5 ha of plantation area were considered to be invaded by plantations; in our dataset, five hectares is the approximate estimated mean size of tree plantations in Africa. We then used high-resolution imagery (see above for methods) to manually inspect all protected areas with >5 ha of plantation expansion, and removed incorrectly predicted plantation polygons from the affected PA's area estimate. To quantify the effect of human influence and accessibility on protected areas, we calculated the maximum human impact index (HII) (*65*) for each protected area and compared the degree of plantation invasion across PAs. The effect of IUCN protected area ranking on the occurrence of plantations in PAs was also examined, across three plantation area thresholds (0, 5 and 50 ha). Due to marked differences in mean IUCN rank across continents and data nonlinearity, we compared the mean IUCN rank between parks with and without plantations (binomial response variable) using Kruskal-Wallis one-way ANOVA tests. Tests were done separately for each continent and threshold.

Declarations

Acknowledgments: We thank R.L. Chazdon, R. Crouzeilles, H.L. Beyer, B.C. Tice, and D. Lagomasino for their contributions to this project's development.

Funding: The authors received no financial support for the research, authorship, and/or publication of this article.

Author contributions: M.E.F.: conceptualization, formal analysis, methodology, validation, visualization, project administration, supervision, and writing; D.H.K.: conceptualization, formal analysis, methodology, and writing; W.S.; validation, L.F.; validation, J.D.; validation, H.C.; validation, J.S.; validation, J.S.; validation, A.T.; methodology, validation, and writing, N.L.H.: resources and writing; E.G.: resources and writing; E.M.O.: resources and writing.

Competing interests: Authors declare no competing interests.

Data and materials availability: All data are available in the main text, online, or in the supplementary materials.

References

1. P. G. Curtis, C. M. Slay, N. L. Harris, A. Tyukavina, M. C. Hansen, Classifying drivers of global forest loss. *Science (80-.).* **361**, 1108–1111 (2018).

2. H. K. Gibbs, A. S. Ruesch, F. Achard, M. K. Clayton, P. Holmgren, N. Ramankutty, J. A. Foley, Tropical forests were the primary sources of new agricultural land in the 1980s and 1990s. *Proc. Natl. Acad. Sci. U. S. A.* **107**, 16732–16737 (2010).

3. T. Payn, J. M. Carnus, P. Freer-Smith, M. Kimberley, W. Kollert, S. Liu, C. Orazio, L. Rodriguez, L. N. Silva, M. J. Wingfield, Changes in planted forests and future global implications. *For. Ecol. Manage.* **352**, 57–67 (2015).

4. F. Pendrill, U. M. Persson, J. Godar, T. Kastner, Deforestation displaced: Trade in forest-risk commodities and the prospects for a global forest transition. *Environ. Res. Lett.* **14**, 055003 (2019).

5. K. Hurni, J. Fox, The expansion of tree-based boom crops in mainland Southeast Asia: 2001 to 2014. *J. Land Use Sci.* **13**, 198–219 (2018).

6. V. Vijay, S. L. Pimm, C. N. Jenkins, S. J. Smith, W. Walker, C. Soto, S. Trigg, D. Gaveau, D. Lawrence, H. Rodrigues, The Impacts of Oil Palm on Recent Deforestation and Biodiversity Loss. **11** (2016) (available at http://dx.plos.org/10.1371/journal.pone.0159668).

7. R. Heilmayr, C. Echeverría, E. F. Lambin, Impacts of Chilean forest subsidies on forest cover, carbon and biodiversity. *Nat. Sustain.* **3**, 701–709 (2020).

8. G. le Maire, S. Dupuy, Y. Nouvellon, R. A. Loos, R. Hakamada, Mapping short-rotation plantations at regional scale using MODIS time series: Case of eucalypt plantations in Brazil. *Remote Sens. Environ.* **152**, 136–149 (2014).

9. M. M. H. Wang, L. R. Carrasco, D. P. Edwards, Reconciling Rubber Expansion with Biodiversity Conservation. *Curr. Biol.* **30**, 3825-3832.e4 (2020).

10. S. L. Lewis, C. E. Wheeler, E. T. A. Mitchard, A. Koch, Restoring natural forests is the best way to remove atmospheric carbon. *Nature*. **568**, 25–28 (2019).

11. R. Dave, C. Saint-Laurent, L. Murray, G. Antunes Daldegan, R. Brouwer, C. A. de Mattos Scaramuzza, L. Raes, S. Simonit, M. Catapan, G. García Contreras, C. Ndoli, A., Karangwa, N. Perera, S. Hingorani, T. Pearson, "Second Bonn Challenge progress report. Application of the Barometer in 2018." (Gland, Switzerland, 2019).

12. S. L. Lewis, C. E. Wheeler, E. T. A. Mitchard, A. Koch, Regenerate natural forests to store carbon. **28**, 25–28 (2019).

13. S. Sloan, P. Meyfroidt, T. K. Rudel, F. Bongers, R. Chazdon, The forest transformation: Planted tree cover and regional dynamics of tree gains and losses. *Glob. Environ. Chang.* **59**, 101988 (2019).

14. R. Petersen, D. Aksenov, E. Esipova, E. D. Goldman, N. Harris, I. Kurakina, T. Loboda, A. Manisha, S. Sargent, V. Shevade, D. Aksenov, A. Manisha, E. Esipova, V. Shevade, T. Loboda, N. Kuksina, Mapping tree plantations with multispectral imagery: preliminary results for seven tropical countries. *World Resour. Institute, Washington, DC*, 1–18 (2016).

15. K.-H. Erb, S. Luyssaert, P. Meyfroidt, J. Pongratz, A. Don, S. Kloster, T. Kuemmerle, T. Fetzel, R. Fuchs, M. Herold, H. Haberl, C. D. Jones, E. Marín-Spiotta, I. McCallum, E. Robertson, V. Seufert, S. Fritz, A. Valade, A. Wiltshire, A. J. Dolman, Land management: data availability and process understanding for global change studies. *Glob. Chang. Biol.* **23**, 512–533 (2017).

16. C. M. Souza, J. Z. Shimbo, M. R. Rosa, L. L. Parente, A. A. Alencar, B. F. T. Rudorff, H. Hasenack, M. Matsumoto, L. G. Ferreira, P. W. M. Souza-Filho, S. W. de Oliveira, W. F. Rocha, A. V Fonseca, C. B. Marques, C. G. Diniz, D. Costa, D. Monteiro, E. R. Rosa, E. Vélez-Martin, E. J. Weber, F. E. B. Lenti, F. F. Paternost, F. G. C. Pareyn, J. V Siqueira, J. L. Viera, L. C. F. Neto, M. M. Saraiva, M. H. Sales, M. P. G. Salgado, R. Vasconcelos, S. Galano, V. V Mesquita, T. Azevedo, Reconstructing Three Decades of Land Use and Land Cover Changes in Brazilian Biomes with Landsat Archive and Earth Engine. *Remote Sens.* . **12** (2020), , doi:10.3390/rs12172735.

17. J. Miettinen, A. Hooijer, C. Shi, D. Tollenaar, R. Vernimmen, S. C. Liew, C. Malins, S. E. Page, Extent of industrial plantations on Southeast Asian peatlands in 2010 with analysis of historical expansion and future projections. *GCB Bioenergy*. **4**, 908–918 (2012).

18. C. Vancutsem, F. Achard, J.-F. Pekel, G. Vieilledent, S. Carboni, D. Simonetti, J. Gallego, L. E. O. C. Aragão, R. Nasi, Long-term (1990–2019) monitoring of forest cover changes in the humid tropics. *Sci. Adv.* **7**, eabe1603 (2021).

19. J.-P. Puyravaud, P. Davidar, W. F. Laurance, Cryptic destruction of India's native forests. *Conserv. Lett.* **3**, 390–394 (2010).

20. M. E. Fagan, D. C. Morton, B. D. Cook, J. Masek, F. Zhao, R. F. Nelson, C. Huang, Mapping pine plantations in the southeastern U.S. using structural, spectral, and temporal remote sensing data. *Remote Sens. Environ.* **216**, 415–426 (2018).

21. R. Tropek, J. Beck, P. Keil, Z. Musilová, Š. Irena, D. Storch, O. Sedláček, J. Beck, P. Keil, Z. Musilová, I. Šímová, D. Storch, Comment on "High-resolution global maps of 21st-century forest cover change." *Sci.* . **344**, 981 (2014).

22. FAO, "Global Forest Resources Assessment 2020" (Rome, 2020).

23. FAO, FAOSTAT agricultural statistics database. (2019), (available at http://faostat.fao.org/site/291/default.aspx).

24. S. C. Cook-Patton, S. M. Leavitt, D. Gibbs, N. L. Harris, K. Lister, K. J. Anderson-Teixeira, R. D. Briggs, R. L. Chazdon, T. W. Crowther, P. W. Ellis, H. P. Griscom, V. Herrmann, K. D. Holl, R. A. Houghton, C. Larrosa, G. Lomax, R. Lucas, P. Madsen, Y. Malhi, A. Paquette, J. D. Parker, K. Paul, D. Routh, S. Roxburgh, S. Saatchi, J. van den Hoogen, W. S. Walker, C. E. Wheeler, S. A. Wood, L. Xu, B. W. Griscom, Mapping carbon accumulation potential from global natural forest regrowth. *Nature*. **585**, 545–550 (2020).

25. K. Hurni, A. Schneider, A. Heinimann, D. H. Nong, J. Fox, Mapping the Expansion of Boom Crops in Mainland Southeast Asia Using Dense Time Stacks of Landsat Data. *Remote Sens.* . **9** (2017), , doi:10.3390/rs9040320.

26. J. Miettinen, C. Shi, S. C. Liew, 2015 Land cover map of Southeast Asia at 250 m spatial resolution. *Remote Sens. Lett.* **7**, 701–710 (2016).

27. N. Torbick, L. Ledoux, W. Salas, M. Zhao, Regional Mapping of Plantation Extent Using Multisensor Imagery. *Remote Sens.* **8** (2016).

28. F. A. Azizan, A. M. Kiloes, I. S. Astuti, A. Abdul Aziz, Application of Optical Remote Sensing in Rubber Plantations: A Systematic Review. *Remote Sens.* . **13** (2021), , doi:10.3390/rs13030429.

29. A. Bégué, D. Arvor, B. Bellon, J. Betbeder, D. De Abelleyra, R. P. D. Ferraz, V. Lebourgeois, C. Lelong, M. Simões, S. R. Verón, Remote Sensing and Cropping Practices: A Review. *Remote Sens.* . **10** (2018), , doi:10.3390/rs10010099.

30. T. Jucker, B. Bongalov, D. F. R. P. Burslem, R. Nilus, M. Dalponte, S. L. Lewis, O. L. Phillips, L. Qie, D. A. Coomes, Topography shapes the structure, composition and function of tropical forest landscapes. *Ecol. Lett.* **21**, 989–1000 (2018).

31. J.-B. Féret, G. P. Asner, Spectroscopic classification of tropical forest species using radiative transfer modeling. *Remote Sens. Environ.* **115**, 2415–2422 (2011).

32. A. Poortinga, K. Tenneson, A. Shapiro, Q. Nquyen, K. San Aung, F. Chishtie, D. Saah, Mapping Plantations in Myanmar by Fusing Landsat-8, Sentinel-2 and Sentinel-1 Data along with Systematic Error Quantification. *Remote Sens.* . **11** (2019), , doi:10.3390/rs11070831.

33. V. H. Gutiérrez-Vélez, R. DeFries, M. Pinedo-Vásquez, M. Uriarte, C. Padoch, W. Baethgen, K. Fernandes, Y. Lim, High-yield oil palm expansion spares land at the expense of forests in the Peruvian Amazon. *Environ. Res. Lett.* **6**, 044029 (2011).

34. A. Descals, S. Wich, E. Meijaard, D. L. A. Gaveau, S. Peedell, Z. Szantoi, High-resolution global map of smallholder and industrial closed-canopy oil palm plantations. *Earth Syst. Sci. Data*. **13**, 1211–1231 (2021).

35. E. M. Ordway, R. L. Naylor, R. N. Nkongho, E. F. Lambin, Oil palm expansion and deforestation in Southwest Cameroon associated with proliferation of informal mills. *Nat. Commun.* **10**, 114 (2019).

36. R. Heilmayr, C. Echeverría, R. Fuentes, E. F. Lambin, A plantation-dominated forest transition in Chile. *Appl. Geogr.* **75**, 71–82 (2016).

37. M. C. Hansen, P. V Potapov, R. Moore, M. Hancher, S. A. Turubanova, A. Tyukavina, D. Thau, S. V Stehman, S. J. Goetz, T. R. Loveland, A. Kommareddy, A. Egorov, L. Chini, C. O. Justice, J. R. G. Townshend, High-resolution global maps of 21st-century forest cover change. *Science (80-.).* **342**, 850–3 (2013).

38. W. J. Bond, N. Stevens, G. F. Midgley, C. E. R. Lehmann, The Trouble with Trees: Afforestation Plans for Africa. *Trends Ecol. Evol.* **34**, 963–965 (2019).

39. J. W. Veldman, G. E. Overbeck, D. Negreiros, G. Mahy, S. Le Stradic, G. W. Fernandes, G. Durigan, E. Buisson, F. E. Putz, W. J. Bond, Where Tree Planting and Forest Expansion are Bad for Biodiversity and Ecosystem Services. *Bioscience*. **65**, 1011–1018 (2015).

40. M. E. Fagan, A lesson unlearned? Underestimating tree cover in drylands biases global restoration maps. *Glob. Chang. Biol.*, 4679– 4690 (2020).

41. M. E. Fagan, J. L. Reid, M. B. Holland, J. G. Drew, R. A. Zahawi, How feasible are global forest restoration commitments? *Conserv. Lett.* **13** (2020), doi:10.1111/conl.12700.

42. A. Malkamäki, D. D'Amato, N. J. Hogarth, M. Kanninen, R. Pirard, A. Toppinen, W. Zhou, A systematic review of the socio-economic impacts of large-scale tree plantations, worldwide. *Glob. Environ. Chang.* **53**, 90–103 (2018).

43. N. B. Schwartz, T. M. Aide, J. Graesser, H. R. Grau, M. Uriarte, Reversals of Reforestation Across Latin America Limit Climate Mitigation Potential of Tropical Forests. *Front. For. Glob. Chang.* **3**, 85 (2020).

44. P. Noojipady, D. C. Morton, W. Schroeder, K. M. Carlson, C. Huang, H. K. Gibbs, D. Burns, N. F. Walker, S. D. Prince, Managing fire risk during drought: the influence of certification and El Niño on fire-driven forest conversion for oil palm in Southeast Asia. *Earth Syst. Dyn. Discuss.*, 1–23 (2017).

45. E. L. Bullock, C. E. Woodcock, C. Souza Jr., P. Olofsson, Satellite-based estimates reveal widespread forest degradation in the Amazon. *Glob. Chang. Biol.* **26**, 2956–2969 (2020).

46. V. H. A. Heinrich, R. Dalagnol, H. L. G. Cassol, T. M. Rosan, C. T. de Almeida, C. H. L. Silva Junior, W. A. Campanharo, J. I. House, S. Sitch, T. C. Hales, M. Adami, L. O. Anderson, L. E. O. C. Aragão, Large carbon sink potential of secondary forests in the Brazilian Amazon to mitigate climate change. *Nat. Commun.* **12**, 1785 (2021).

47. P. Potapov, X. Li, A. Hernandez-Serna, A. Tyukavina, M. C. Hansen, A. Kommareddy, A. Pickens, S. Turubanova, H. Tang, C. E. Silva, J. Armston, R. Dubayah, J. B. Blair, M. Hofton, Mapping global forest canopy height through integration of GEDI and Landsat data. *Remote Sens. Environ.* **253**, 112165 (2021).

48. B. Bernal, L. T. Murray, T. R. H. Pearson, Global carbon dioxide removal rates from forest landscape restoration activities. *Carbon Balance Manag.* **13**, 22 (2018).

49. R. Heilmayr, C. Echeverría, E. F. Lambin, Impacts of Chilean forest subsidies on forest cover, carbon and biodiversity. *Nat. Sustain.* **3**, 701–709 (2020).

50. W. Li, M. F. Goodchild, R. Church, An efficient measure of compactness for two-dimensional shapes and its application in regionalization problems. *Int. J. Geogr. Inf. Sci.* **27**, 1227–1250 (2013).

51. G. P. Asner, Cloud cover in Landsat observations of the Brazilian Amazon. *Int. J. Remote Sens.* **22**, 3855–3862 (2001).

52. A. M. Wilson, W. Jetz, Remotely Sensed High-Resolution Global Cloud Dynamics for Predicting Ecosystem and Biodiversity Distributions. *PLoS Biol.* **14**, e1002415 (2016).

53. V. H. Gutiérrez-Vélez, R. DeFries, Annual multi-resolution detection of land cover conversion to oil palm in the Peruvian Amazon. *Remote Sens. Environ.* **129**, 154–167 (2013).

54. J. Reiche, R. Lucas, A. L. Mitchell, J. Verbesselt, D. H. Hoekman, J. Haarpaintner, J. M. Kellndorfer, A. Rosenqvist, E. A. Lehmann, C. E. Woodcock, F. M. Seifert, M. Herold, Combining satellite data for better tropical forest monitoring. *Nat. Clim. Chang.* **6**, 120–122 (2016).

55. J. J. Erinjery, M. Singh, R. Kent, Mapping and assessment of vegetation types in the tropical rainforests of the Western Ghats using multispectral Sentinel-2 and SAR Sentinel-1 satellite imagery. *Remote Sens. Environ.* **216**, 345–354 (2018).

56. M. Shimada, T. Itoh, T. Motooka, M. Watanabe, T. Shiraishi, R. Thapa, R. Lucas, New global forest/non-forest maps from ALOS PALSAR data (2007–2010). *Remote Sens. Environ.* **155**, 13–31 (2014).

57. R. Torres, P. Snoeij, D. Geudtner, D. Bibby, M. Davidson, E. Attema, P. Potin, B. Rommen, N. Floury, M. Brown, GMES Sentinel-1 mission. *Remote Sens. Environ.* **120**, 9–24 (2012).

58. P. Potapov, M. C. Hansen, L. Laestadius, S. Turubanova, A. Yaroshenko, C. Thies, W. Smith, I. Zhuravleva, A. Komarova, S. Minnemeyer, E. Esipova, The last frontiers of wilderness: Tracking loss of intact forest landscapes from 2000 to 2013. *Sci. Adv.* **3**, e1600821 (2017).

59. UNEP-WCMC, "World Database on Protected Areas User Manual 1.4 (downloaded 10-18)" (Cambridge, UK., 2016).

60. H2O, AutoML: Automatic Machine Learning (2020), (available at https://h2o-release.s3.amazonaws.com/h2o/rel-yau/5/docs-website/h2o-docs/automl.html).

61. S. P. Healey, W. B. Cohen, Z. Yang, C. Kenneth Brewer, E. B. Brooks, N. Gorelick, A. J. Hernandez, C. Huang, M. Joseph Hughes, R. E. Kennedy, T. R. Loveland, G. G. Moisen, T. A. Schroeder, S. V Stehman, J. E. Vogelmann, C. E. Woodcock, L. Yang, Z. Zhu, Mapping forest change using stacked generalization: An ensemble approach. *Remote Sens. Environ.* **204**, 717–728 (2018).

62. D. Lagomasino, T. Fatoyinbo, S. Lee, E. Feliciano, C. Trettin, A. Shapiro, M. M. Mangora, Measuring mangrove carbon loss and gain in deltas. *Environ. Res. Lett.* **14**, 25002 (2019).

63. P. Bunting, A. Rosenqvist, R. M. Lucas, L.-M. Rebelo, L. Hilarides, N. Thomas, A. Hardy, T. Itoh, M. Shimada, C. M. Finlayson, The global mangrove watch—a new 2010 global baseline of mangrove extent. *Remote Sens.* **10**, 1669 (2018).

64. A. H. Pickens, M. C. Hansen, M. Hancher, S. V Stehman, A. Tyukavina, P. Potapov, B. Marroquin, Z. Sherani, Mapping and sampling to characterize global inland water dynamics from 1999 to 2018 with full Landsat time-series. *Remote Sens. Environ.* **243**, 111792 (2020).

65. O. Venter, E. W. Sanderson, A. Magrach, J. R. Allan, J. Beher, K. R. Jones, H. P. Possingham, W. F. Laurance, P. Wood, B. M. Fekete, M. A. Levy, J. E. M. Watson, Global terrestrial Human Footprint maps for 1993 and 2009. *Sci. Data*. **3**, 160067 (2016).

66. GADM, Database of Global Administrative Areas (GADM) v3.6 (2018), (available at https://gadm.org/download_country_v3.html).

67. R. J. Hijmans, E. Williams, C. Vennes, M. R. J. Hijmans, Package 'geosphere.' *Spherical Trigonometry*. **1** (2017).

68. D. M. Olson, E. Dinerstein, E. D. Wikramanayake, N. D. Burgess, G. V. N. Powell, E. C. Underwood, J. A. D'amico, I. Itoua, H. E. Strand, J. C. Morrison, Terrestrial Ecoregions of the World: A New Map of Life on Earth: A new global map of terrestrial ecoregions provides an innovative tool for conserving biodiversity. *Bioscience*. **51**, 933–938 (2001).

69. R. A. Mittermeier, W. R. Turner, F. W. Larsen, T. M. Brooks, C. Gascon, in *Biodiversity hotspots* (Springer, Berlin, Heidelberg, 2011), pp. 3–22.

70. P. Potapov, M. C. Hansen, L. Laestadius, S. Turubanova, A. Yaroshenko, C. Thies, W. Smith, I. Zhuravleva, A. Komarova, S. Minnemeyer, E. Esipova, The last frontiers of wilderness : Tracking loss of intact forest landscapes from 2000 to 2013, 1–14 (2017).

Figures

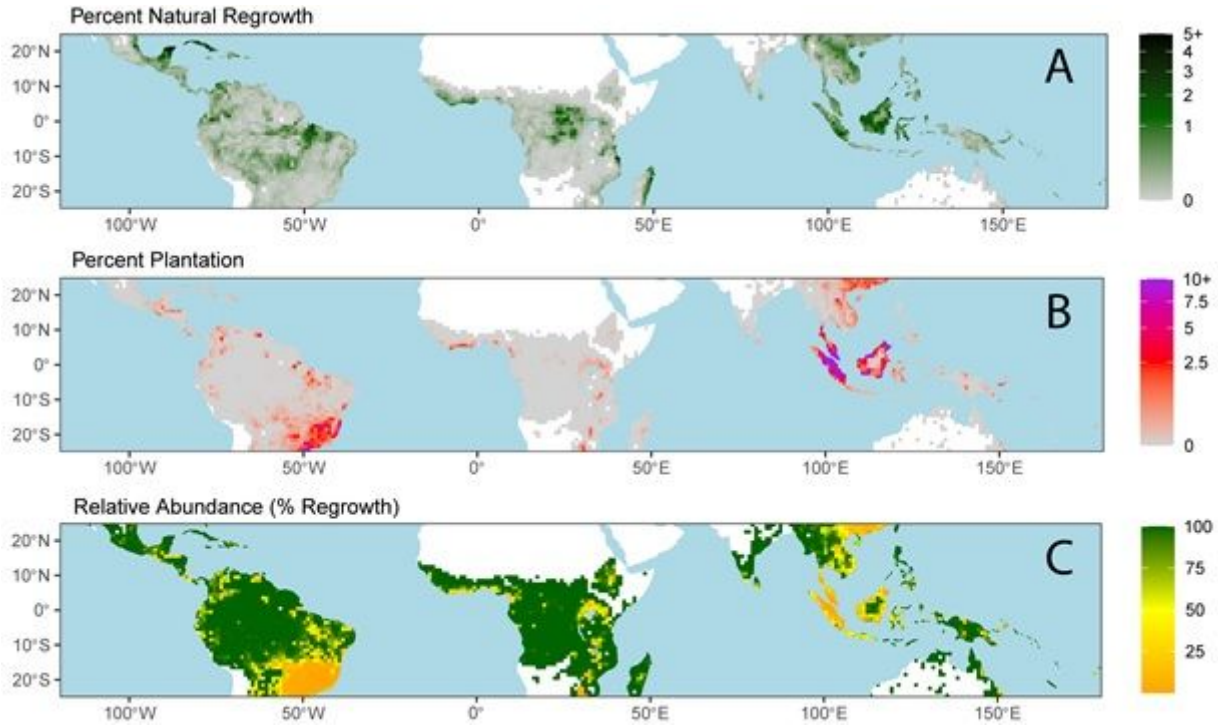

Figure 1

Pantropical distribution of natural regrowth and tree plantations. Higher-resolution (30 m) data were summed across one-degree grid cells for display; the percent land area occupied by each land use class is shown in panels A and B. In panel C, the relative abundance of natural regrowth is shown, as a proportion of total gains in tree cover. Note: The designations employed and the presentation of the material on this map do not imply the expression of any opinion whatsoever on the part of Research

Square concerning the legal status of any country, territory, city or area or of its authorities, or concerning the delimitation of its frontiers or boundaries. This map has been provided by the authors.

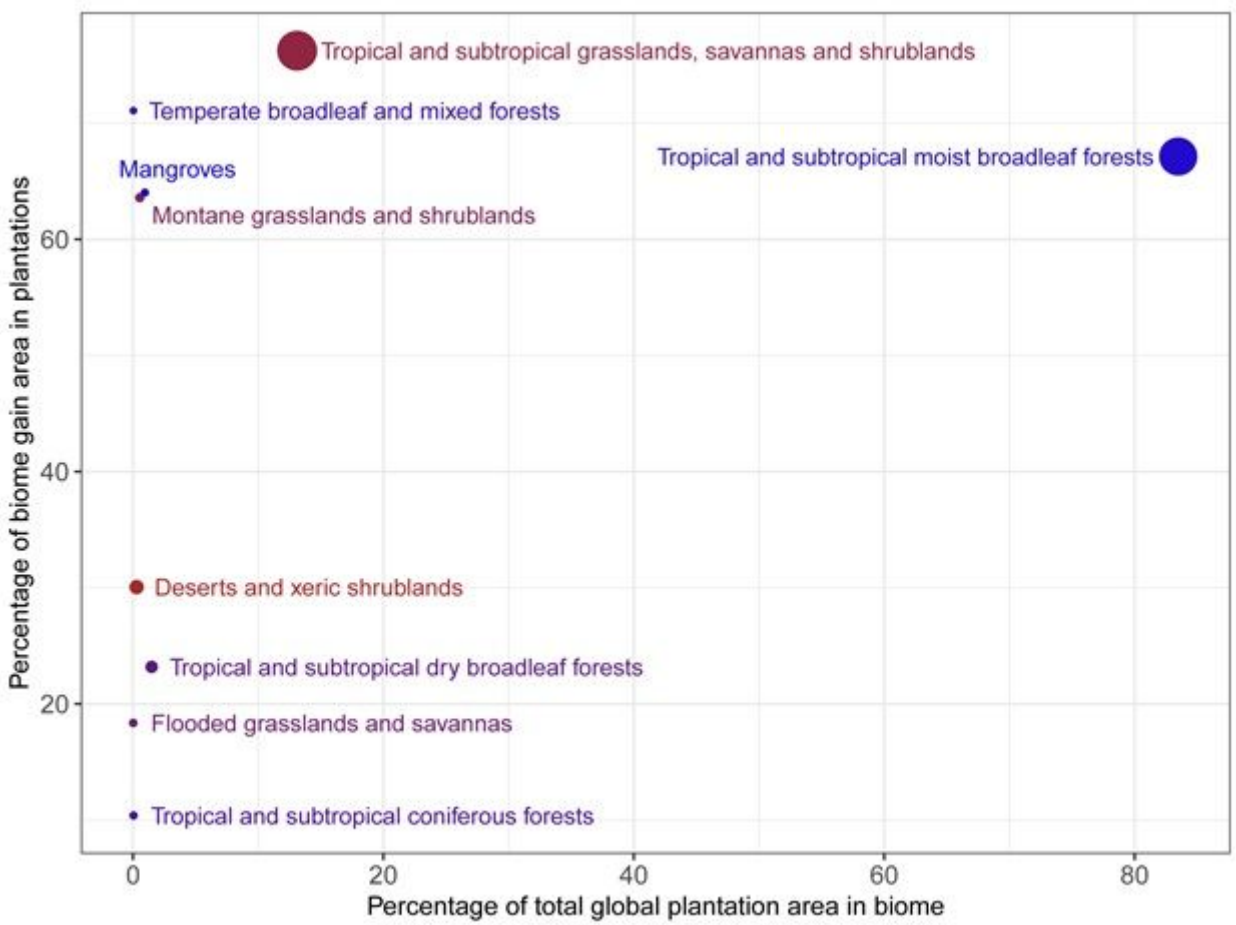

Figure 2

Proportional expansion of tree plantations into terrestrial biomes. Points are colored by biome aridity, from blue (humid) to brown (arid), and point size is scaled to tropical biome area. Temperate forest biomes were located in tropical montane regions. Data shown is normalized biome plantation area, both as a percentage of total global plantation area (x-axis), and as a percentage of total tree cover gain in each biome (y-axis).

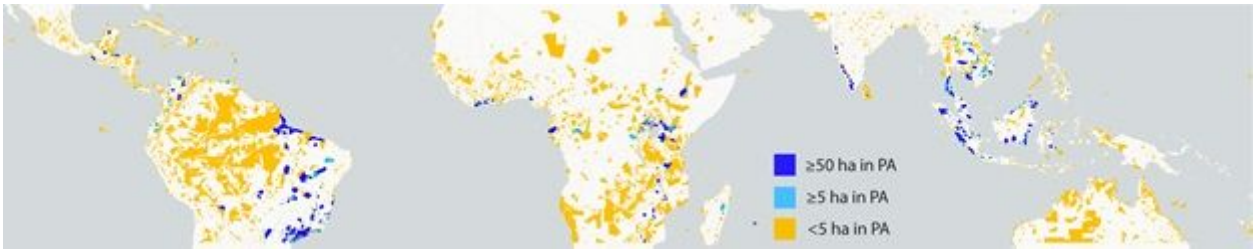

Figure 3

Expansion of plantations into tropical protected areas. Protected areas (PAs) are color-coded by estimated plantation expansion area (2000-2012). Note: The designations employed and the presentation of the material on this map do not imply the expression of any opinion whatsoever on the part of

Research Square concerning the legal status of any country, territory, city or area or of its authorities, or concerning the delimitation of its frontiers or boundaries. This map has been provided by the authors.

Supplementary Files

This is a list of supplementary files associated with this preprint. Click to download.

- NatureSustSupplementaryMaterialsFaganetalv10.docx
- Nature2021Fagantestfin111520allClocsXYselected.csv
- Nature2021FaganLUCassess3000randPtshumidTropics060621v1.csv